

AFRL-IF-RS-TR-2004-95
Final Technical Report
April 2004



PUPIL PLANE ARRAY BASED MILLIMETER- WAVE IMAGING RADIOMETER

Trex Enterprises Corporation

APPROVED FOR PUBLIC RELEASE; DISTRIBUTION UNLIMITED.

**AIR FORCE RESEARCH LABORATORY
INFORMATION DIRECTORATE
ROME RESEARCH SITE
ROME, NEW YORK**

STINFO FINAL REPORT

This report has been reviewed by the Air Force Research Laboratory, Information Directorate, Public Affairs Office (IFOIPA) and is releasable to the National Technical Information Service (NTIS). At NTIS it will be releasable to the general public, including foreign nations.

AFRL-IF-RS-TR-2004-95 has been reviewed and is approved for publication.

APPROVED:

/s/
PETER J. COSTIANES
Project Engineer

FOR THE DIRECTOR:

/s/
JOSEPH CAMERA, Chief
Information & Intelligence Exploitation Division
Information Directorate

| REPORT DOCUMENTATION PAGE | | | Form Approved OMB No. 074-0188 | |
|---|--|---|---|---|
| Public reporting burden for this collection of information is estimated to average 1 hour per response, including the time for reviewing instructions, searching existing data sources, gathering and maintaining the data needed, and completing and reviewing this collection of information. Send comments regarding this burden estimate or any other aspect of this collection of information, including suggestions for reducing this burden to Washington Headquarters Services, Directorate for Information Operations and Reports, 1215 Jefferson Davis Highway, Suite 1204, Arlington, VA 22202-4302, and to the Office of Management and Budget, Paperwork Reduction Project (0704-0188), Washington, DC 20503 | | | | |
| 1. AGENCY USE ONLY (Leave blank) | | 2. REPORT DATE April 2004 | | 3. REPORT TYPE AND DATES COVERED Final Aug 01 – Feb 03 |
| 4. TITLE AND SUBTITLE PUPIL PLANE ARRAY BASED MILLIMETER-WAVE IMAGING RADIOMETER | | | 5. FUNDING NUMBERS C - F30602-01-C-0154 PE - N/A PR - CWDP TA - 00 WU - 06 | |
| 6. AUTHOR(S) Stuart Clark, John Lovberg, Vladimir Kolinko, Chris Martin, John McCoy | | | | |
| 7. PERFORMING ORGANIZATION NAME(S) AND ADDRESS(ES) Trex Enterprises Corporation 10455 Pacific Center Court San Diego CA 92121-4339 | | | 8. PERFORMING ORGANIZATION REPORT NUMBER N/A | |
| 9. SPONSORING / MONITORING AGENCY NAME(S) AND ADDRESS(ES) AFRL/IFEC 32 Brooks Road Rome NY 13441-4114 | | | 10. SPONSORING / MONITORING AGENCY REPORT NUMBER AFRL-IF-RS-TR-2004-95 | |
| 11. SUPPLEMENTARY NOTES AFRL Project Engineer: Peter J. Costianes/IFEC/(315) 330-4030 Peter.Costianes@rl.af.mil | | | | |
| 12a. DISTRIBUTION / AVAILABILITY STATEMENT APPROVED FOR PUBLIC RELEASE; DISTRIBUTION UNLIMITED. | | | | 12b. DISTRIBUTION CODE |
| 13. ABSTRACT (Maximum 200 Words) The work performed under this contract was related to the testing and procurement of the phase and, in particular, frequency processor boards that are needed in Trex Enterprises' second generation real-time passive millimeter-wave camera (PMC). In addition, an imaging demonstration performed under this contract demonstrated the feasibility of building such a PMC and that it is possible to obtain near diffraction limited imagery. The Trex Enterprises Corporation's PMC imager uses a patented flat panel antenna and millimeter-wave signal processors to enable a 30 by 20 degree instantaneous field of view true real time (30 Hz) sensor with a 2 Kelvin instantaneous thermal sensitivity, to be built in a highly compact package suitable for concealed weapons detection. The millimeter-wave (MMW) portion of the electromagnetic spectrum is chosen as it offers a good balance between clothing penetration as well as resolution and, therefore, allows compact, practical sized systems suitable for law enforcement to be built. By measuring only natural thermal emissions (from living beings and inanimate objects), and reflections of natural ambient sources (such as the cold sky), passive millimeter-wave imaging is intrinsically safe and suitable for imaging people. | | | | |
| 14. SUBJECT TERMS Passive Millimeter Wave Sensor, Low Noise Amplifier, Rotman Lens, Concealed Weapons Detection | | | | 15. NUMBER OF PAGES 28 |
| | | | | 16. PRICE CODE |
| 17. SECURITY CLASSIFICATION OF REPORT UNCLASSIFIED | 18. SECURITY CLASSIFICATION OF THIS PAGE UNCLASSIFIED | 19. SECURITY CLASSIFICATION OF ABSTRACT UNCLASSIFIED | 20. LIMITATION OF ABSTRACT UL | |

Table of Contents

| | | |
|------------|--|-----------|
| 1.0 | INTRODUCTION | 1 |
| 2.0 | THEORY OF OPERATION..... | 1 |
| 2.1 | ANTENNA | 5 |
| 2.2 | OCTAPAKS & AMPLIFIERS | 7 |
| 2.3 | PROCESSORS | 10 |
| 2.3.1 | <i>Phase Processor</i> | <i>10</i> |
| 2.3.2 | <i>Frequency Processor.....</i> | <i>11</i> |
| 2.3.3 | <i>Processor Board Manufacture.....</i> | <i>12</i> |
| 2.3.4 | <i>Frequency Processor Board components.....</i> | <i>13</i> |
| 2.4 | DATA ACQUISITION SYSTEM | 14 |
| 3.0 | COMPONENT DEVELOPMENT | 14 |
| 3.1 | PHASE PROCESSOR | 14 |
| 3.2 | FREQUENCY PROCESSOR | 17 |
| 4.0 | FRONT END DEMO..... | 20 |
| 5.0 | CONCLUSIONS | 23 |

List of Figures

| | |
|--|----|
| Figure 1. (Left) Front view of the PMC-2 imager showing where the patented flat panel antenna is placed. (Right) Rear view showing power supplies and the area where the frequency processor cassette will go. | 1 |
| Figure 2. PMC-2 Imaging Concept..... | 3 |
| Figure 3. PMC-2 System Flowchart..... | 3 |
| Figure 4. PMC-2 Physical System Assembly Concept..... | 4 |
| Figure 5. PMC-2 Physical Components Assembly Drawing..... | 4 |
| Figure 6a. WR-10 waveguide to W-band receiver. | 5 |
| Figure 6b. PMC-2 parallel plate waveguide antenna. | 6 |
| Figure 6c. The principle of the slotted antenna. | 6 |
| Figure 7. Computer modeling of slotted antenna..... | 7 |
| Figure 8. Schematic and performance of a receiver channel..... | 8 |
| Figure 9a. Photograph of completed PMC-2 Octapak. | 9 |
| Figure 9b. Octapak gain and noise figure data while running at typical drain bias | 9 |
| Figure 10. This shows a first generation X band Rotman Lens | 10 |
| Figure 11. PMC-2 phase processor design with 232 input channels, 192 output channels and input bootlace | 11 |
| Figure 12. PMC-2 Frequency Processor. | 12 |
| Figure 13. Schematic of the board structure..... | 13 |
| Figure 14. High magnification picture of W-band detector diode from HRL. | 13 |
| Figure 15. PMC-2 phase processor board with attached transitions to allow testing..... | 15 |
| Figure 16. Phase processor test results showing the variation in input phase slope with output channel | 16 |
| Figure 17. By measuring the phase at output port 153 out of a total of 192 output ports, and comparing to the expected theoretical phase, tests have confirmed that the residual phase errors are within acceptable limits and are of order 0.1 waves. | 16 |
| Figure 18. Simulations have shown that errors with a standard deviation of less than 45 degrees (upper right) have little effect on image quality. | 17 |
| Figure 19. Frequency processor test board with probe output to test functionality of lens and feed structures without the complication of actual diodes being present..... | 18 |
| Figure 20. Response of probe based test boards..... | 18 |
| Figure 21. Full frequency processor board including W-band detector diodes..... | 19 |
| Figure 22. Response of full frequency processor board including W-band detector diodes. Note the near “sinc squared” type of response (point spread function). | 19 |
| Figure 23. Images of the PMC-2 front end used for the front end demo..... | 20 |
| Figure 24. Before and after phaseup response functions at mid band and mid field of view..... | 21 |
| Figure 25a. Antenna pattern, $f=83$ GHz, output 112. | 22 |
| Figure 25b. Antenna pattern, $f=93$ GHz, output 145. | 22 |
| Figure 25c. Antenna pattern, $f=77$ GHz, output 169. | 23 |
| Figure 25d. Antenna pattern, $f=85$ GHz, output 33. | 23 |

1.0 INTRODUCTION

This contract which was a follow-on to two previous National Institute of Justice (NIJ) grants (grant numbers 97-LB-VX-K015 and 98-DT-CX-K006), was aimed at providing NIJ through Air Force Rome Labs, Information Directorate (AFRL-ID) with a second generation passive millimeter-wave camera (PMC) suitable for real time concealed weapons detection (CWD).

The proposed system known as PMC-2 (Figure 1) uses Trex Enterprises Corporation's (Trex) patented flat panel antenna and millimeter-wave signal processors to enable a 30 by 20 degree instantaneous field of view true real time (30 Hz) sensor with a 2 Kelvin instantaneous thermal sensitivity, to be built in a portable 2 foot square by 10 inch deep package.

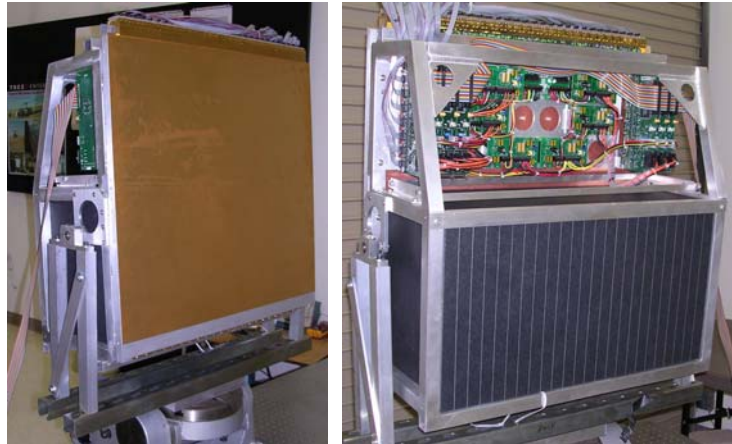


Figure 1. (Left) Front view of the PMC-2 imager showing where the patented flat panel antenna is placed. (Right) Rear view showing power supplies and the area where the frequency processor cassette will go.

The millimeter-wave (MMW) portion of the electromagnetic spectrum is chosen as it offers a good balance between clothing penetration as well as resolution and therefore allows compact, practical sized systems suitable for law enforcement to be built. By measuring only natural thermal emissions (from living beings and inanimate objects), and reflections of natural ambient sources (such as the cold sky), passive millimeter-wave imaging is intrinsically safe and suitable for imaging people. Indeed it is worth noting that outdoors, reflection of the cold sky (i.e. deep space background at an effective temperature of about 70K at W band on a clear day) is the dominant detected signal.

The PMC-2 imager uses a novel frequency scanned phased array flat panel antenna coupled to MMW low noise amplifiers (LNAs), to produce enough signal to allow a two-dimensional MMW Rotman lens (comprised of one phase processor and 192 frequency processors), to perform the Fourier transform that is needed to go from the antenna (pupil plane) to the image plane. Custom detector diodes and A/D chips are then used to detect and digitize the image plane MMW signal. The digitized signal is then fed to a high performance PC for processing and display.

2.0 THEORY OF OPERATION

As a result of its heritage in aviation where weight and space are of critical importance, PMC-2 uses a very novel approach to passive millimeter-wave imaging that allows small compact form

factors but at the expense of some added complexity in how the imager works. This section will describe in significant detail how the imager works by starting with the antenna and following the incident signal through the signal all the way to the detector diodes and image processing software.

Traditional MMW imagers, i.e. so called focal plane arrays require not only a large volume but an excessive number of expensive RF amplifiers. The large volume arises from the fact that in general, due to aberrations, one does not want to make the focal length of the system less than the diameter of the lens being used to collect the incident signals. Since for resolution reasons most MMW systems need collection apertures of 2 to 4 ft, this would result in focal lengths of at least this and thus leads to systems of very large volume. The large number of amplifiers arises from the fact that at MMW, current state of the art detectors are not sensitive enough to detect natural thermal emissions without a large amount (30 to 50 dB) of amplification (gain) prior to detection with the result that one is faced with putting amplifiers on each and every detector. When this is coupled with the fact that in a reasonable field of view (FOV) such as 30 by 20 degrees, there are some 25,000 pixels, it leads to an excessive number of expensive and difficult to obtain RF amplifiers being required.

To try and overcome these inherent limitations, Trex Enterprises developed a novel imaging approach based upon so called pupil plane imaging. In pupil plane imaging, one typically uses an array of small receivers that detect the far field signal of the object in question, and then a Fourier Transform (FT) is applied to the detected signal to form the image. Since there is no longer the need to focus the detected signal onto the array elements, pupil plane imagers typically have very little depth to them and thus need far less volume than a focal plane system. As an example, consider PMC-2 which has a 2ft square aperture, but needs only 10 inches of depth.

In current pupil plane imagers such as phased arrays (X band or lower frequency) operated by such entities as DoD, the FT is today performed using high speed digital electronics. However in the case of PMC-2 since it operates from 75 to 93 GHz, i.e. too fast for digital electronics, other methods must be found. The method ultimately selected by Trex is based upon an old technology known as a Rotman Lens that uses a metal layer on a dielectric substrate with curved input and output surfaces (much like a cylindrical lens in visible optics) to perform a 1-dimensional FT. An introduction to Rotman Lenses can be found in the book "Phased Array Antennas" page 341 by R. C. Hansen (ISBN 0-471-53076-X)

A second key part of PMC-2 is the novel patented flat panel antenna that Trex developed and that serves as the array of small receivers normally associated with pupil plane imagers. This antenna, which will be described in more detail later in this section, maps position to phase in the horizontal direction (i.e. functions as a conventional phased array in this direction). However in the vertical direction, the antenna uses a position to frequency mapping. To better understand this, consider an optical diffraction grating illuminated with white light. On the output side, one sees distinct colors at well defined viewing angles. By reciprocity, if a white source is located at an angle to the grating, then only a particular narrowband color will pass through the grating. This is exactly the case with PMC-2 where we are dealing with all sorts of natural (broadband) sources in the field of view. For each elevation, the antenna will only pass (respond) to one particular narrowband signal and thus we have an effective one to one elevation to frequency mapping. As a result of its operation, the antenna is referred to as a frequency scanned phased array antenna.

In addition, by the nature of its design and how many slots and output holes are cut into it, the antenna allows the incident signal to be channelized, i.e. broken up into discrete separate channels

(232 in this case) that can then be individually amplified. This last step is critical since there is currently no way to amplify a spatially continuous signal, it must be broken down in to discrete channels that can be fed to amplifiers whose input (typically a small waveguide) is less than a wavelength in size.

Since the antenna uses different mechanisms to scan each direction, the FT that is required can be broken down into two sequential 1-d transforms using different Rotman lenses that Trex refers to as the phase and frequency processors.

Having completed the above basic introduction to pupil plane imagers, we can now conceptually layout the operation of the PMC-2 imager as shown in Figure 2.

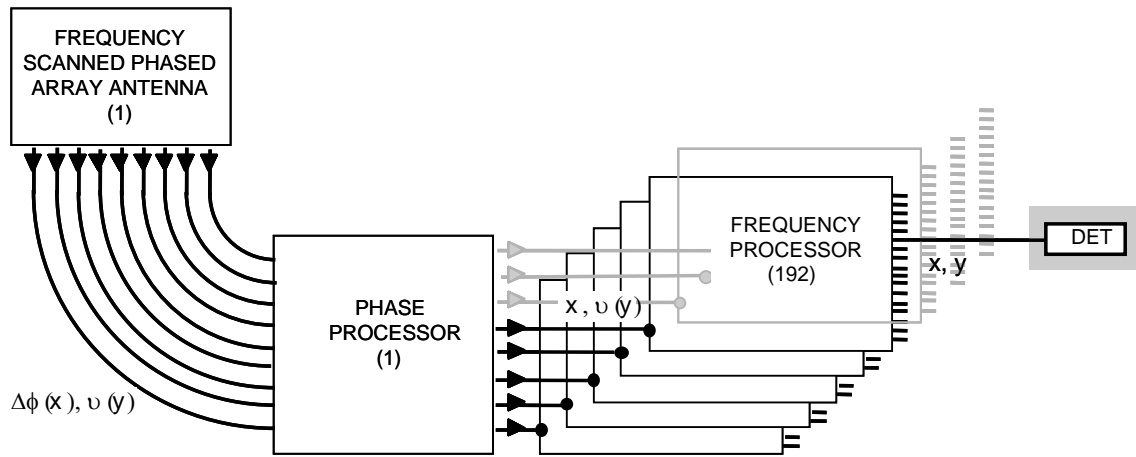


Figure 2. PMC-2 Imaging Concept. With the Trex approach, image reconstruction is split into 2 phases. A single phase processor is used to remove the position to phase mapping and in so doing, organize the data into columns. Multiple frequency processors (192 in this case) each of which has multiple detector diodes (128 in this case) are then used on a column by column basis to remove the position to frequency mapping in the vertical direction and form a 2 dimensional image of 192 by 128 pixels.

This concept translates to the following system flowchart shown in Figure 3 and the physical implementation shown in Figures 4 and 5.

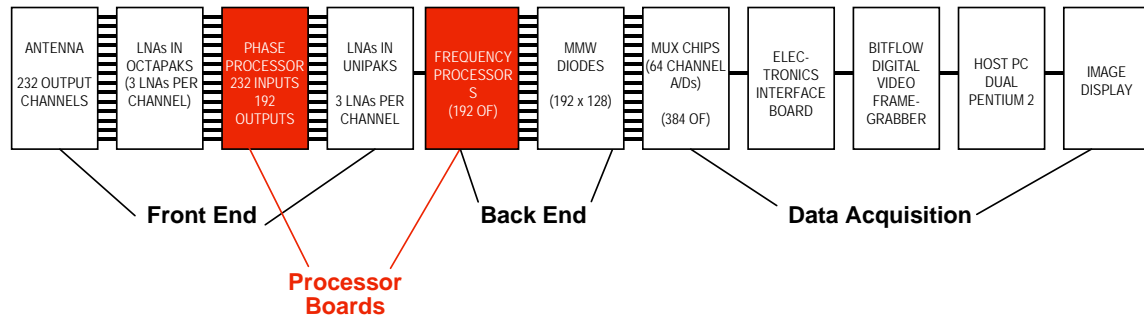


Figure 3. PMC-2 System Flowchart showing the various sections of the imager from front to back and can be broken down into three main sections (front end, back end and data acquisition) together with various sub-sections.

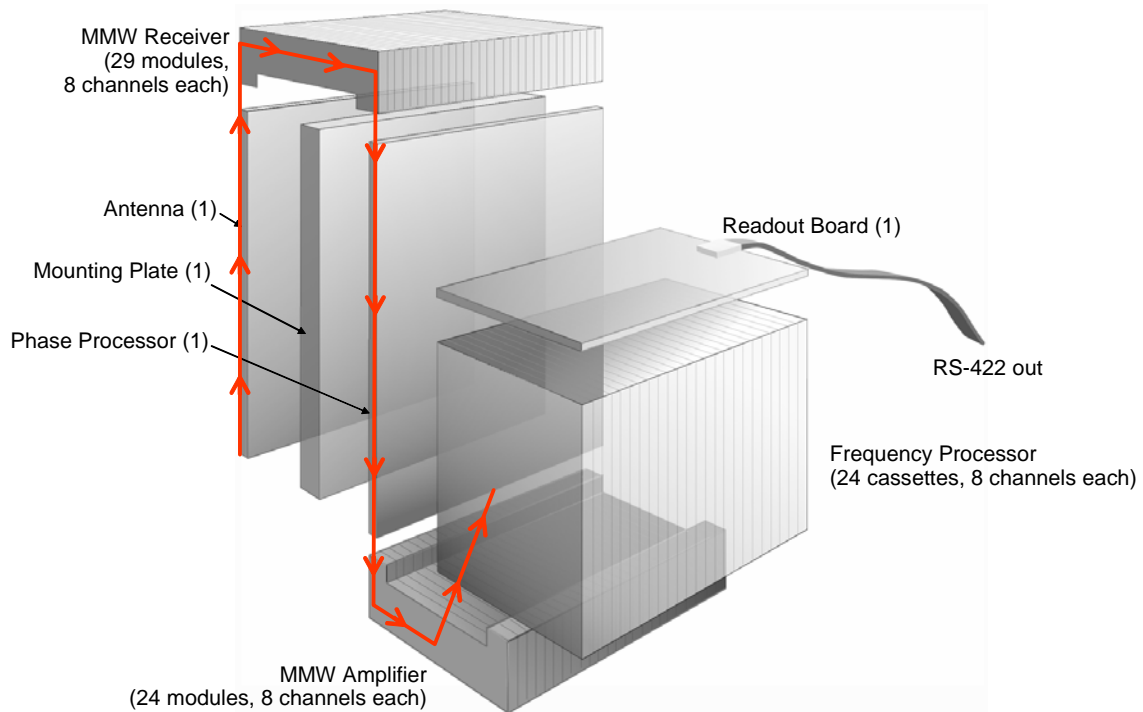


Figure 4. PMC-2 Physical System Assembly Concept. This figure can be used to show how the MMW signal (shown in red) flows through PMC-2 by starting at the antenna and tracing a path up and through the front end amplifiers, down and through the phase processor, through the back end amplifiers and then up and into the frequency processor cassettes (each holding 8 frequency processor boards) where the detector diodes convert the MMW signal into a DC voltage that can be measured.

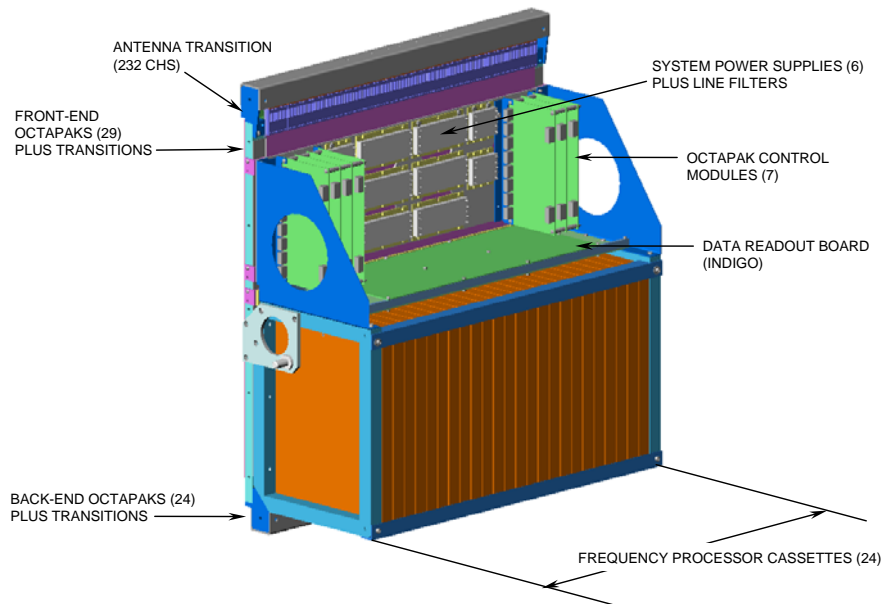


Figure 5. PMC-2 Physical Components Assembly Drawing. In addition to the individual components, this figure shows the system support rack, SSR (in blue in the above figure) that is used to provide string rigid mount points.

Based upon the fact that the imager is in reality the combination of an antenna, some amplifiers and the custom processor boards followed by a high performance PC, the following sub-sections will describe the components of the imager working sequentially from front to back.

2.1 Antenna

Developed under IR&D funding and awarded US patent # 6,037,908, Trex Enterprises' flat panel MMW antenna is a lightweight planar antenna designed for high gain at extremely low cost. The antenna (Figure 6) is composed of a single sheet of 30-mil-thick polyethylene dielectric, with copper cladding on both sides and a sequence of small slots photolithographically etched on one side. As a result of this, the antenna can be thought of (and behaves as) a parallel plate dielectric filled waveguide, with the top and bottom copper cladding (sheets) acting as the waveguide (albeit a very big flat waveguide) and the polyethylene acting as a dielectric filler material. A TEM-mode traveling wave propagates within the antenna's parallel-plate dielectric-filled waveguide.

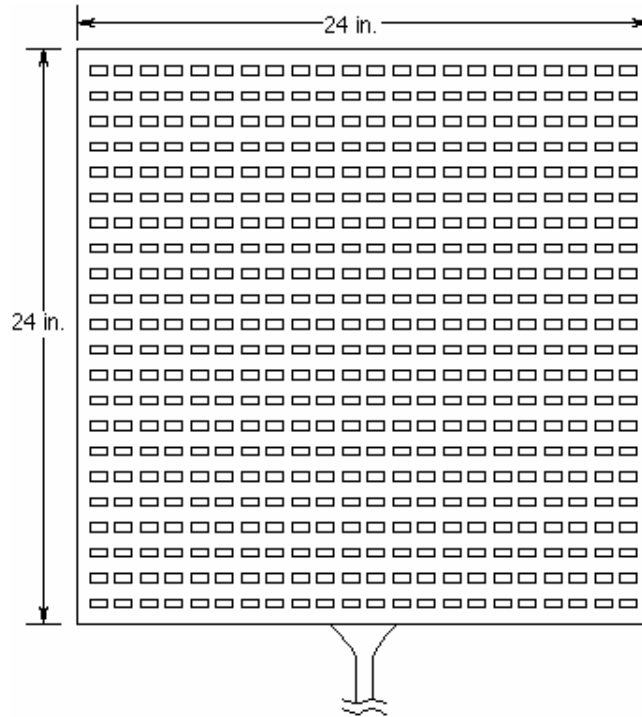


Figure 6a. WR-10 waveguide to W-band receiver. Parallel plate waveguide with 30 mil polyethylene dielectric sandwiched between two copper sheets. Note only a single feed is shown; in general a phased array of such feeds spans the lower edge of the antenna, for imaging or radar applications.

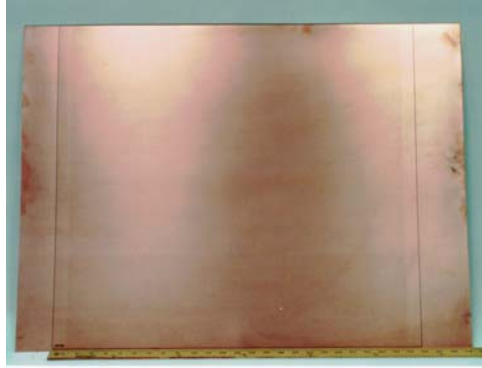


Figure 6b. *PMC-2 parallel plate waveguide antenna.*

In general the antenna was designed by use of reciprocity i.e. it was for mathematical convenience treated as an emitter, which in practice meant treating the antenna as if there was a wave propagating in it that had to get out into free space. Using this analogy coupled with concepts from geometrical optics provides a powerful framework to describe, model and design the antenna in.

In order for the wave inside the antenna to get out, there must be some type of opening in the antenna. In the Trex antenna, the openings are provided by rectangular slots, the spacing of which can be derived analytically (as shown below) while the slot width has been empirically determined based upon PMC-1 and numerous experiments by Trex over the last several years.

If the slots are too large, not only will there coupling be very frequency dependent i.e. not broadband response, but they will let out the energy so fast that little if any energy will propagate to the slots furthest from the feed and in effect reduce the operating size and thus resolution of the antenna. On the other hand if the slots are too narrow little energy will be able to couple in and so the antenna will have a much higher loss associated with it. After considerable work, a width in the range 32 to 33 mils was determined to be optimal.

To determine the slot spacing, the slots should be thought of as individual sources with a certain phase and strength whose power combines constructively or destructively in the far field depending on the direction. Figure 6c illustrates the geometry for calculating the angle θ of the main beam.

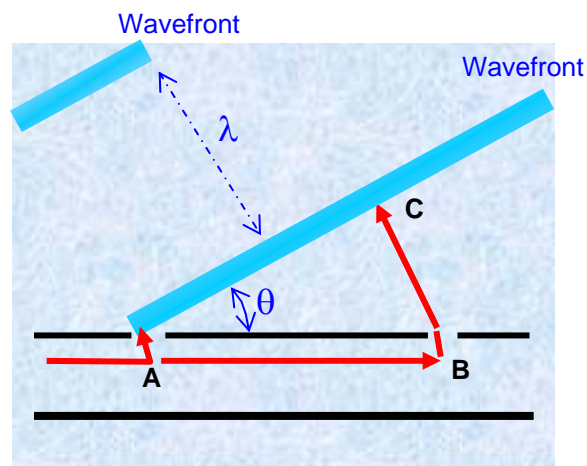


Figure 6c. *The principle of the slotted antenna.*

Two adjacent slots A and B are shown. Distance AB between slots will be denoted as d , wavelength in the air as λ , index of refraction of the antenna dielectric as n and angle of propagation as θ . In order for the waves emitted from slots A and B to combine constructively in direction determined by the angle θ the following condition must be met:

$$n \cdot d \cdot \sin(\theta) = \lambda \cdot k \quad \text{where } k=0, \pm 1, \pm 2 \dots$$

The above equation states that the optical path length difference between the two waves in direction given by θ must be equal to an integer number of the wavelengths. Because wavelength λ enters the equation it is clear that the main beam angle will vary with frequency. Given values of n , d and λ , angle θ can be found:

$$\theta = \arcsin(\lambda / d \cdot k \cdot n)$$

As is typical in these cases, the slot spacing should be such that $k = 1$ is the only mode that can exist otherwise there would be multiple beams and complete confusion as to where a signal originated from. Using $\lambda = 139$ mil (corresponding to the frequency 85 GHz), $n=1.55$ (polyethylene) and $d = 78$ mils the antenna will form a single beam at $\theta = 13.43$ degrees. When signal frequency varies from 75 GHz to 95 GHz the main beam angle scans from 28.0 to 2.56 degrees. As this range of angles falls within the PMC design goals, the slot spacing was indeed set to 78 mils.

Figure 7 below shows the result of RF modeling of the Trex antenna and confirms via reciprocity that a wave incident at an angle to the antenna is transformed into a wave traveling inside and parallel to the antenna.

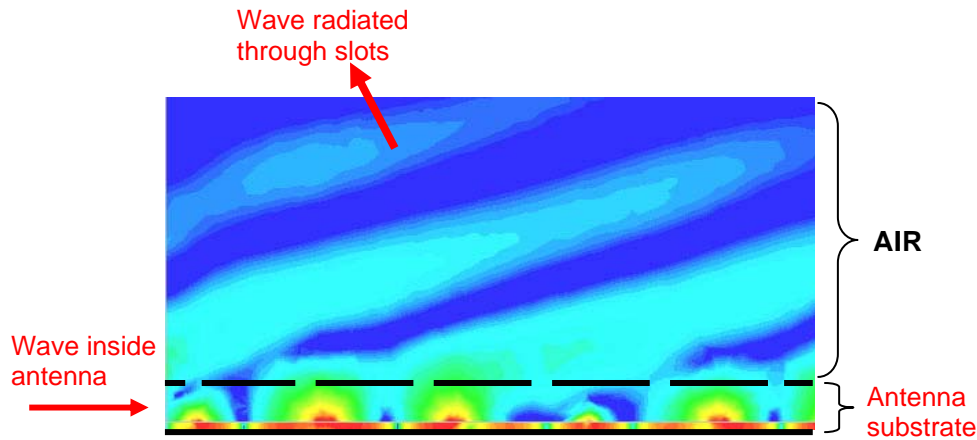
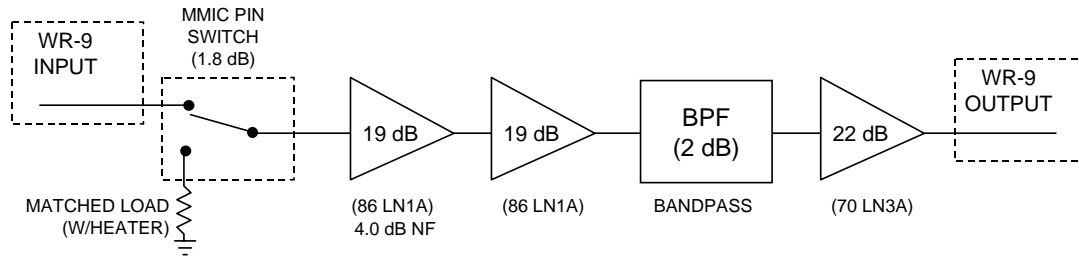


Figure 7. Computer modeling of slotted antenna.

2.2 Octapaks & Amplifiers

As is customary in radiometric systems, the signal received by the antenna must be amplified so that it can efficiently and reasonably be detected above the background noise that is intrinsic to such signals. In order to perform the amplification, the antenna output is as previously discussed broken into many independent channels (232 in total) since there is no technology that can amplify the continuum of signals that a 2-foot wide antenna produces.

Complicating the design is the very limited space available to put 232 separate amplifier channels into especially when one realizes that in traditional approaches, each amplifier channel is placed inside its own metal box so as to minimize cross talk etc. The solution to this problem was to place 8 channels worth of components within a single package (known as an Octapak) that is approximately 0.9 by 1 inches in size. Given the proximity of high gain components, this approach required considerable work to eliminate cross-talk and ringing. The former of which was especially hard as each amplifier channel is made up of 3 individual low noise amplifier (LNA) chips that each have about 20 dB of gain for a combined typical gain (after inter-connection losses) of around 55dB.



Goals:

- ◆ > 53 dB small-signal gain
- ◆ 86 GHz center frequency
- ◆ 18 GHz bandwidth
- ◆ < 6 dB noise figure
- ◆ ± 3 dB gain flatness
- ◆ Output power (P_{1dB}) > 0 dBm

Results Summary (to date):

55.0 dB
84.5 GHz
18 GHz
6.8 dB
 ± 4 dB max
0 dBm

Figure 8. Schematic and performance of a receiver channel.

The basic amplifier layout is shown in Figure 8 above and includes the 3 stage LNA chain coupled to a bandpass filter and PIN switch that is used to perform the Dicke switching required for system calibration and in particular, the flat fielding.

The actual LNAs are state-of-the-art InP devices built for Trex by HRL Laboratories. Of the two final designs (86LN1A and 70LN3A) produced, the 86LN1A chip had lower noise figure performance (typically 3.5 dB vs. 4.0 dB) while the 70LN3A design chip provided a higher output power level (typically 0 dBm vs. -6 dBm). The performance goals for the low noise amplifiers delivered by HRL Laboratories are as follows:

- Average gain of 19 dB min. within 75.5 to 93.5 GHz band;
- Gain flatness of ± 3.0 dB max. within band;
- Noise figure less than 4.5 dB within band; and,
- Input and output return loss each less than -2 dB within band.

Independently run tests on sample chips from each wafer, performed by Jet Propulsion Laboratory (JPL) for Trex Enterprises, confirmed that the LNA performance for both designs was in accordance with performance goals above.

Once delivered, the individual LNA chips were assembled into the Octapak modules. Based upon the performance of each design, each channel typically consists of one 86LN1A chip as the first amplifier followed by two 70LN3A chips. The 86LN1A is used first as it has the lower noise figure and overall system noise figure is largely set by the first amplification stage. The 70LN3A chips are used to provide enough power to the MMW detector diodes to ensure that the imager is thermal noise not detector noise limited.

It should be noted that due to the losses in the phase and frequency processors, the MMW signals must be amplified at both the input and output of the phase processor. Doing this ensures that the signal entering the frequency processor (about 0 dBm) is sufficient to drive the diodes in a regime where thermal noise not diode and or A/D noise is the dominant noise source. This ensures that we are getting the best temperature resolution possible, limited only by the noise level in the MMW amplifiers which are currently the best anywhere in the world.

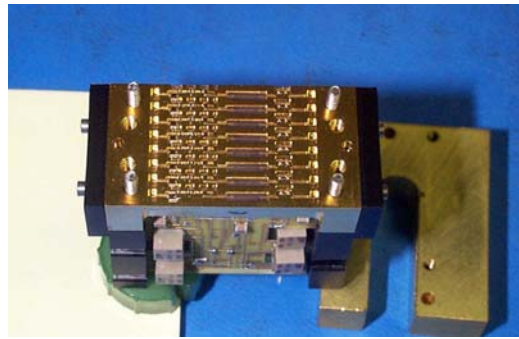


Figure 9a. Photograph of completed PMC-2 Octapak. This photo was taken looking at the top-side of the unit and shows the 8 individual amplifier channels. The large grayish section in the center of the image is the bandpass filter and there are 2 stages of amplification before the filter (i.e. to the left) and 1 after (to the right).

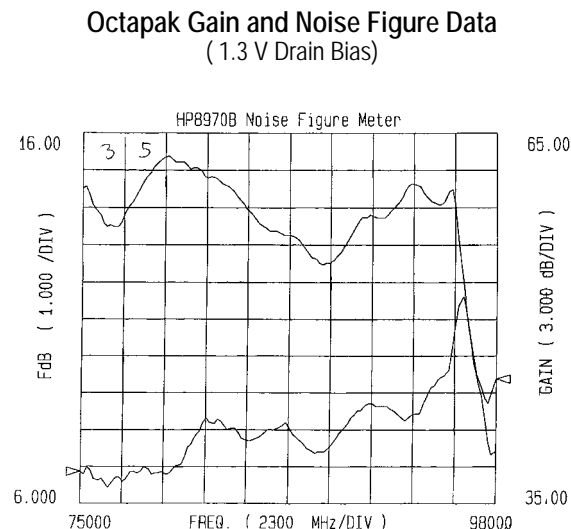


Figure 9b. Octapak gain and noise figure data while running at typical drain bias. The upper graph represents the gain across the band and uses the scale on the right hand side of the graph which corresponds to 5 dB of gain per vertical division. The lower curve represents the noise figure of the Octapak across the band and uses the scale on the left of the graph, which corresponds to 1 dB increments per vertical division.

2.3 Processors

A Rotman lens upon which the phase and frequency processors are based, is in its simplest form (Figure 10) is simply an appropriately shaped metal layer on a dielectric substrate. The curved surfaces may be thought of as serving the same function as the curved surfaces of a cylindrical optical lens. Just as in optics, by appropriately selecting the curvature of each metal edge, a Fourier transform type relationship can be setup between input and output surfaces.

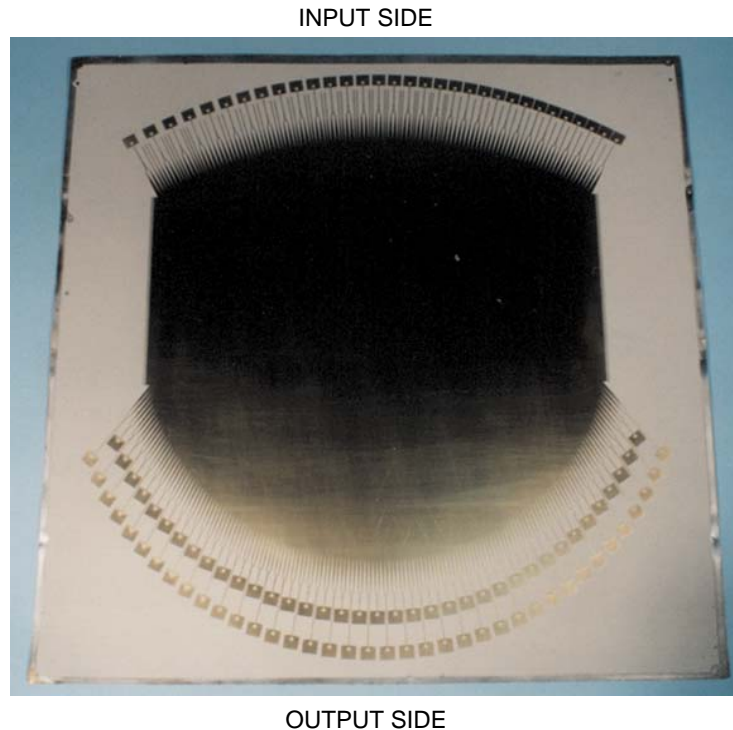


Figure 10. This shows a first generation X band Rotman Lens. Notice the curved input and output surfaces that when coupled with the large area of metal in the middle of the lens allows a Fourier Transform type relationship to exist between input and output sides of the lens

Since the phase and frequency processors respectively remove the azimuthal-position to phase and elevation-position to frequency mappings, they are sufficiently different that they need to be described in separate sections prior to discussing the materials and techniques actually used to make the boards.

2.3.1 Phase Processor

For a Rotman lens to be a phase processor (Figure 11) i.e. to perform the phase based transform that is needed in the horizontal direction to remove the position to phase mapping that the antenna applies to the incident MMW signal, two things must occur.

- A) The number of phase processor input channels must match the number of antenna output channels (232) in this case AND
- B) The output from each channel on the antenna must be connected to the phase processor such that the phase pattern at the antenna output is maintained to the input of the lens section of the processor.

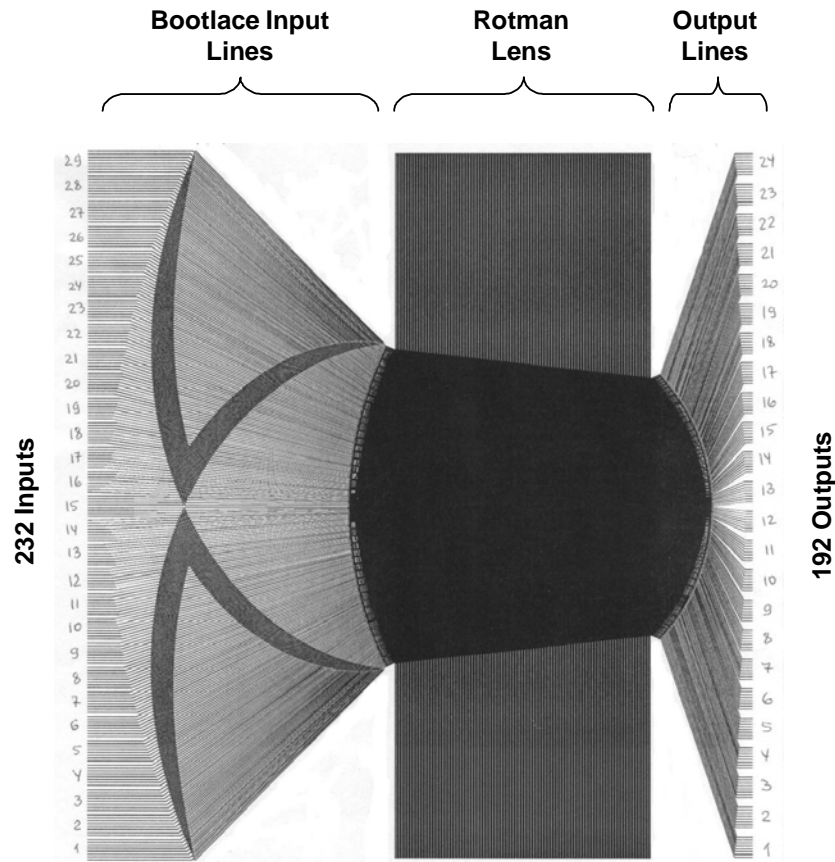


Figure 11. *PMC-2 phase processor design with 232 input channels, 192 output channels and input bootlace*

While matching the number of antenna and input phase processor channels is simple, maintaining the phase pattern requires ensuring that for each signal line, the pathlength from the input of the phase processor (along the straight edge of the board) to the point where it touches the curved lens is the same. This is done by using what is called a bootlace on the actual phase processor board. A bootlace is simply a circuit design feature where the line length is varied by serpentineing each line so that the total length from input to the lens is the same no matter where on the curved input surface the input port is located.

2.3.2 Frequency Processor

For a Rotman lens to be a frequency processor (Figure 12) i.e. to be able to remove the position to frequency mapping that the antenna applies in the vertical direction to the incident MMW signal, and since a Rotman Lens works on phase (as do optical lenses), a way must be found to convert a frequency based mapping back to a phase based mapping. This is done by adding a tapped delay line section added to the input side of the lens.

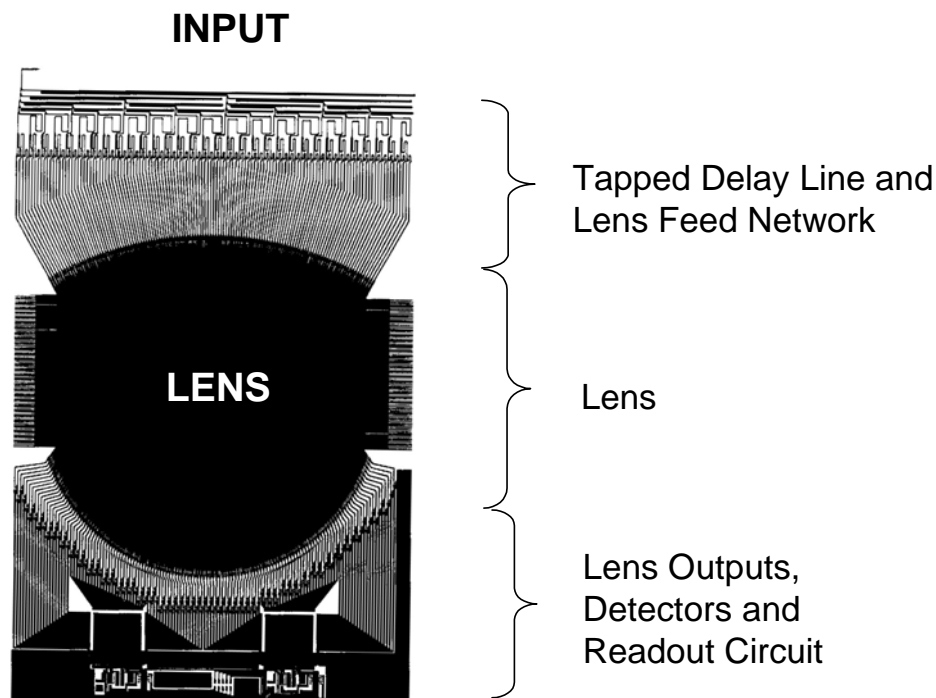


Figure 12. PMC-2 Frequency Processor showing the tapped delay line input at the top of the Rotman Lens, the Rotman itself and the output detector diodes and miscellaneous components.

In this approach, the path (time delay) to each input port is linearly increased from the first port to the last port by a distance which is some multiple (in this case 3x) of the center wavelength for the frequency band of interest. By doing this, the phase between ports linearly increases or decreases as the incident signal moves above or below the design center frequency and as a result, we have converted a frequency related effect into a phase effect. Thus just as with an optical lens, this linear change in phase looks to the lens like an off axis object and thus frequencies above or below the design center frequency will be steered to off axis output ports

2.3.3 Processor Board Manufacture

Due to the exotic materials required to keep the MMW losses low enough, actually producing the phase and frequency processors boards is a huge undertaking in and of itself. Due to the high losses of most circuit board materials at W-band, the best existing material commercially available had a loss per inch that was more than twice what initial calculations showed could be tolerated. In other words, current materials had about 20 dB too much loss. After considerable effort, Trex in collaboration with Sheldahl Inc of Northfield, MN (who also build the boards) developed a di-clad material that consisted of low loss polypropylene sandwiched between sheets of half ounce (0.7 mil thick) rolled (ultra smooth) copper sheeting.

To reduce RF interference and provide mechanical stability, a symmetric sandwich like structure (Figure 13) for the boards was developed. In this approach, two di-clads are melt laminated together with on one board, the entire inner copper layer removed and on the inner layer of the other board, the Rotman lens structure etched into it.

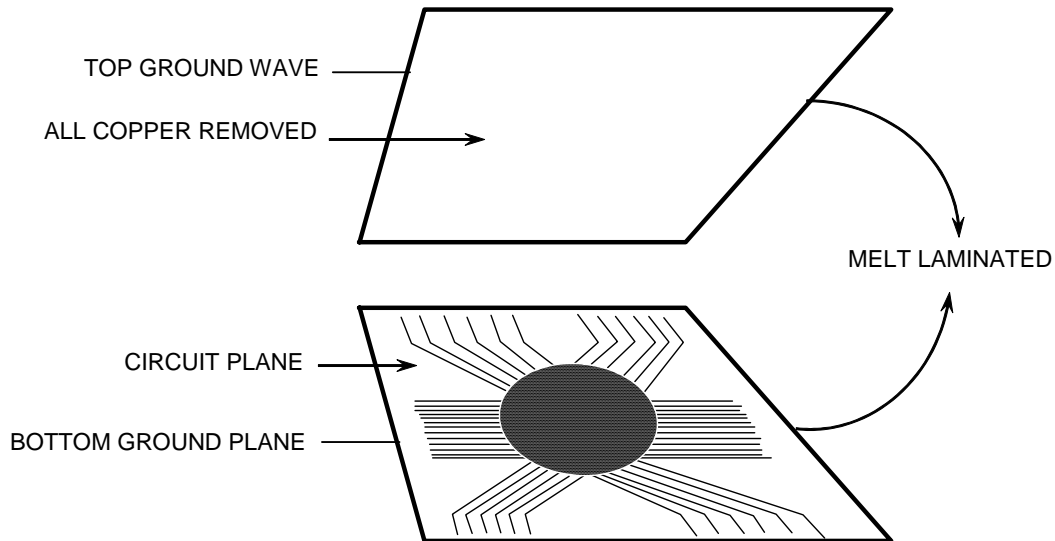


Figure 13. Schematic of the board structure.

2.3.4 Frequency Processor Board components

On the output side of the frequency processor board, MMW detector diodes are required to convert the MMW signal (90+ GHz) into a near-dc-voltage that can actually be measured and digitized. The detector diodes (Figure 14) are highly custom parts made by HRL Laboratories and based on vertical AlSb heterostructures.

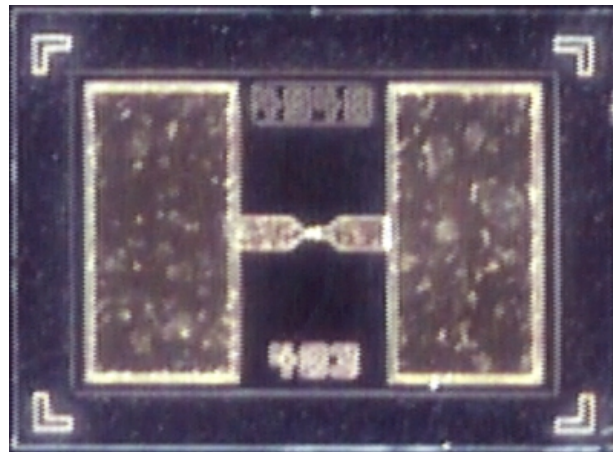


Figure 14. High magnification picture of W-band detector diode from HRL.

The near-DC signal produced by the detector diodes is digitized, using a custom 64-channel 7-bit (instantaneous) ultra low noise MUX chip built for Trex by Indigo Systems of Santa Barbara, CA. To improve performance and substantially reduce cost, the chip was designed with a 7-bit digitizer and a sampling time of 1/64th of a standard 33 ms frame, i.e. approximately 0.5 ms per sampling interval. By using 63 of the possible 64 sampling intervals that are present in a standard 33ms (30 Hz) frame, the output signal resolution is effectively increased to 10 bits. Data is

transferred from buffers on the chip to a readout board during the remaining sampling interval. A custom readout board that takes the parallel outputs from the 384 MUX chips that are present in a PMC-2 imager and converts it to a single serial output in RS-422 digital video format was designed and built by Indigo Systems. This readout board makes extensive use of FPGA chips to buffer and then re-format the parallel signals into a single serial signal.

2.4 Data Acquisition System

To allow for a degree of sensor fusion and for comparison purposes, the ability to simultaneously capture MMW, visible and IR images of the same scene taken at the same time is built into PMC-2 by using RS-422 compatible digital visible and IR cameras. Digital framegrabber boards from Bitflow Corp of Boston, MA coupled with appropriate software from Bitflow and Microsoft is then used to run a custom C based program developed by Trex to control all aspects of the imager.

The imager code which runs to tens of thousands of lines of code, runs under Windows NT. Due to the loading that the three data streams places on the PCI bus that is currently standard on PC's, the PC that controls the PMC has two independent PCI buses and four processors. The code, which is multi-threaded, allows for each sensor's data to be acquired and processed on its own processor, with one processor left to actually display the data via calls to the appropriate windows API functions. Standard and custom real-time algorithms for various calibration and image processing functions have been developed and implemented as part of the code.

3.0 COMPONENT DEVELOPMENT

At the outset of not only this contract but the preceding two NIJ grants that this work was based on, it was agreed that for financial reasons, the CWD program would leverage as much as possible a large concurrent Department of Defense (DOD) program that was aimed at building a PMC-2 imager for the US Army. This DOD program was run by Army Research Laboratory (ARL) in Adelphi, MD (under contracts DAAL01-94-C-0100 and DAA017-01-C-0009) and aimed at providing all weather flight capabilities, primarily to Army helicopters.

Thus the work performed on this contract was related to the testing and procurement of the phase and in particular, frequency processor boards that are required to transform the signals received by the antenna into a final image.

3.1 Phase Processor

As Sheldahl delivered each revision of the phase processor, the boards were initially first tested for electrical continuity of all the traces. This is particularly important on the output side of the lens where losing a trace results in an entire column of pixels being lost. On the input side due to the nature of a pupil plane system (which resembles a Hologram in many ways), losing a trace merely lowers the overall power and image contrast by the ratio of numbers of bad traces to the total number (232) of traces. The RF testing (Figure 15) of the boards involves injecting a known signal on each trace in turn and mapping the power and phase that is received from this input signal on the other side of the lens. The further off center the signal is injected, the larger linear phase variation we should see as this is how as lens works.

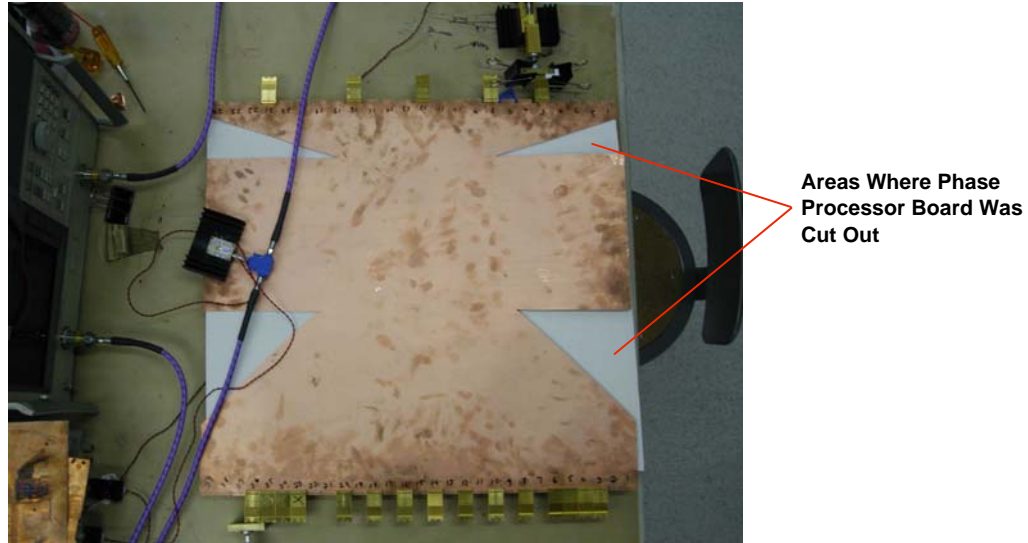


Figure 15. PMC-2 phase processor board with attached transitions to allow testing.
Only the solid copper top ground plane is evident as the signal layer is embedded between this plane and a bottom ground plane.

However as Trex gained more experience with the boards it became clear that there was some sort of interference effect occurring in the board as measurements showed periodic like variations in the transmitted power and phase. Attempts to model such a large device using the generally accept tool i.e. Ansoft's HFSS software were severely hindered by a build up of computation errors that is intrinsic to these iterative software modeling packages when the grid size gets too big, typically more than a few tens of thousands of mesh points. The results from HFSS hinted at a very strange propagation mode that totally ignored the middle signal plane and went between the top and bottom ground planes. Based on this information and since it was clear that the undesirable mode required "line of sight", i.e. a direct path of continuous conductor to reach the output of the board, it was decided to try and block any direct paths from one side of the board to the other by 2 methods.

As shown in Figure 11 there are 4 triangular shaped areas of the board adjacent to the center of the lens (that shows up as the solid black rectangle in the center of Figure 11) and next to the anti-reflection edge treatment that do not have any signal traces in them. These areas as shown in Figure 15 were removed to block any direct input to output signal paths for channels near the edges of the board. In the center of the board, it is clearly impossible to block the direct input to output path as the desired signal must travel this route. To minimize the interference effects, small holes were drilled through the board between each input trace and back filled with absorber. By doing this it is estimated that we attenuate the unwanted propagation mode by 10dB while leaving the desired mode unchanged.

As a result of these 2 methods, it has been possible to bring the performance of the phase processor up to the expected levels and in doing so, produce near diffraction limited performance as is indicated in Figures 16, 17 & 18.

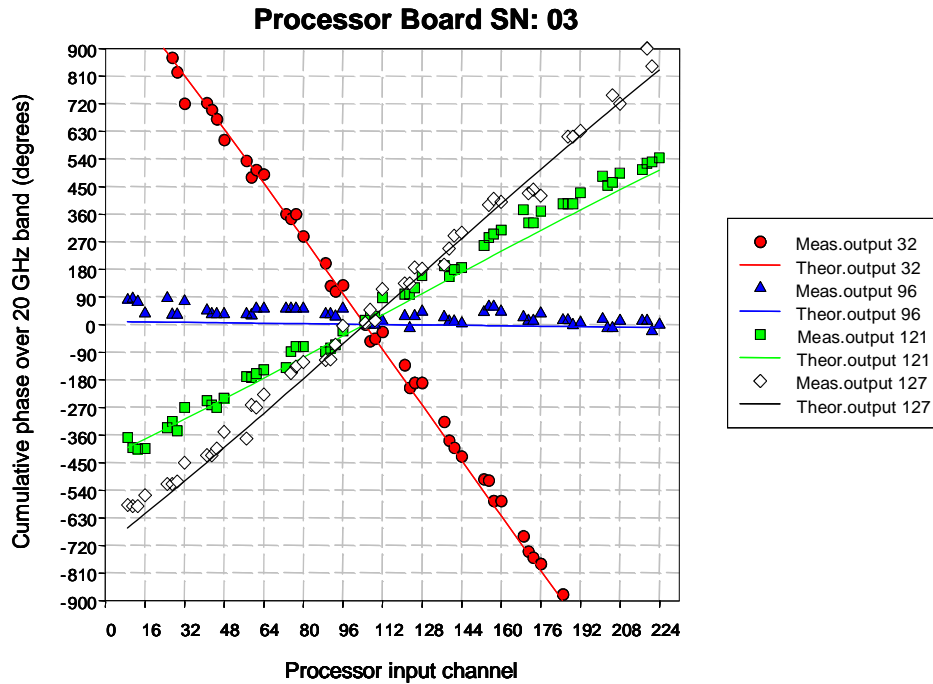


Figure 16. Phase processor test results showing the variation in input phase slope with output channel. It should be noted that on the input side to the phase processor there are 232 channels but only 192 on the output side. The figure shows the phase response of the phase processor at selected output ports (32 96, 121 and 127) and is meant to show typically data rather than all 192 possible data outputs.

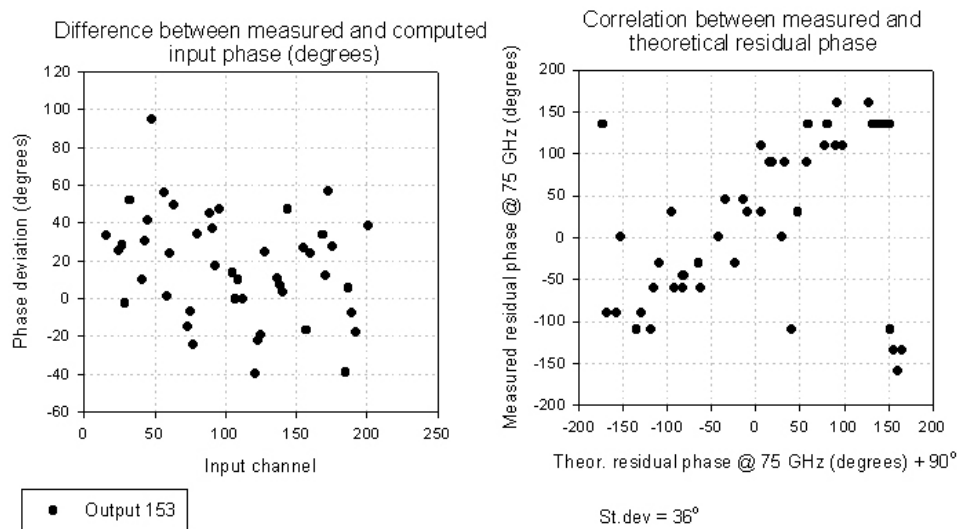


Figure 17. By measuring the phase at output port 153 out of a total of 192 output ports, and comparing to the expected theoretical phase, tests have confirmed that the residual phase errors are within acceptable limits and are of order 0.1 waves.

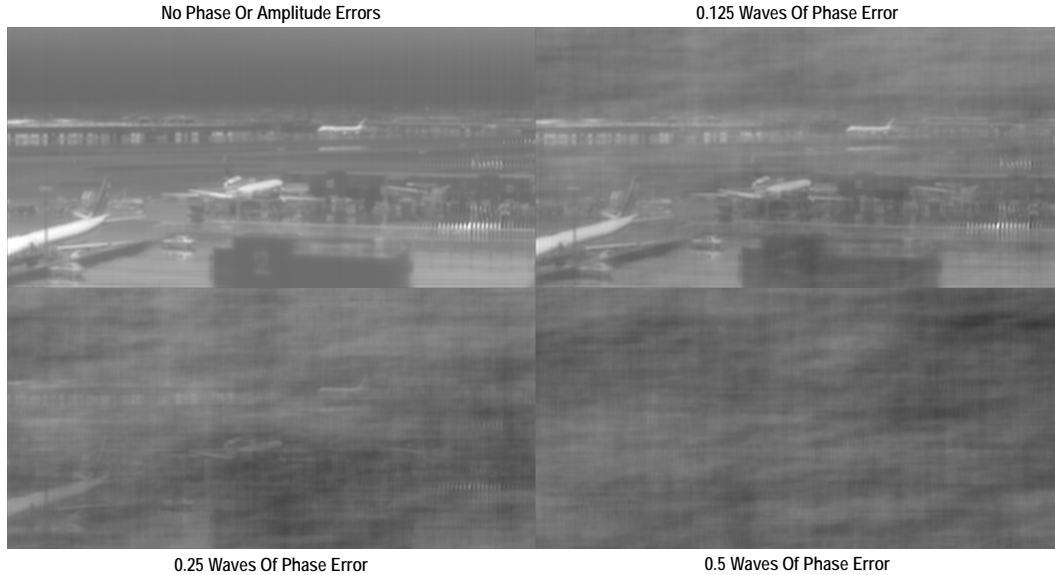


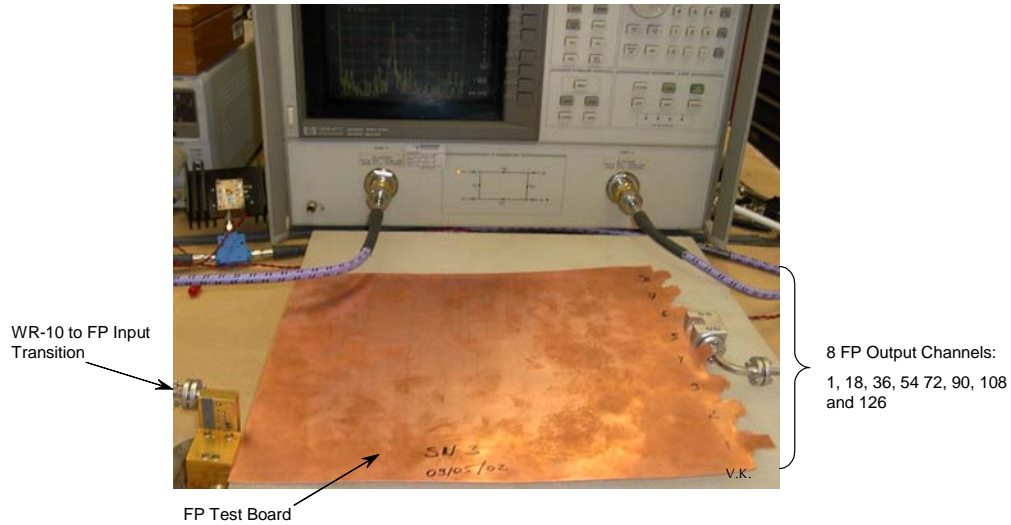
Figure 18. Simulations have shown that errors with a standard deviation of less than 45 degrees (upper right) have little effect on image quality.

Based upon these results, Trex has concluded that it has phase processor boards with acceptable performance.

3.2 Frequency Processor

Since the same vendor is making both the phase and frequency processor boards and based upon a generally agreed assumption that the phase processor was the more difficult of the two boards (principally due to its size of approximately 24 by 22 inches), work was delayed on the frequency processor until one acceptable phase processor had been made.

Testing of the frequency processor board involved inserting a source signal of known amplitude and frequency into the board and measuring the output response of the board at each of the 128 channels. In theory a perfect (i.e. diffraction limited) board would produce the classic “sinc squared” output in response to a single frequency input that is within its pass band of 75 to 93 GHz.



- ◆ Three FP test boards without diodes were made to verify performance of the feed network and the lens

Figure 19. Frequency processor test board with probe output to test functionality of lens and feed structures without the complication of actual diodes being present.

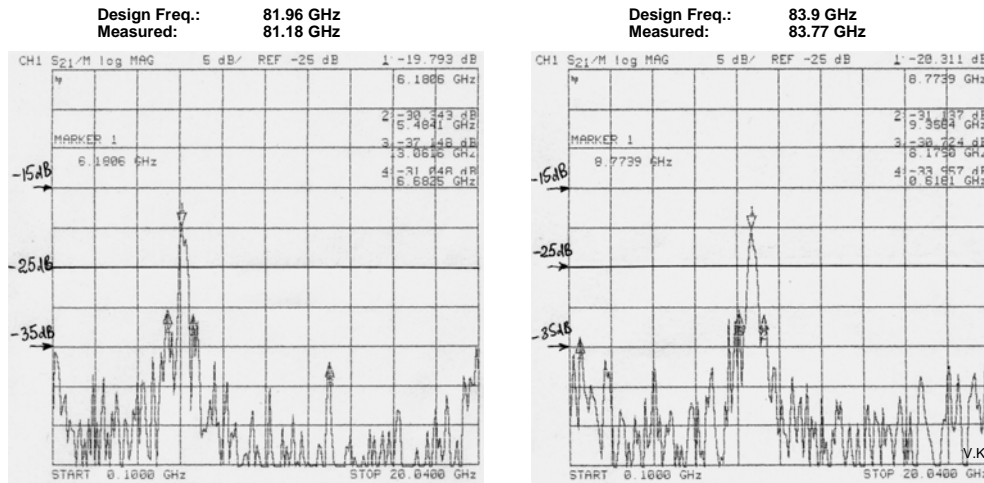


Figure 20. Response of probe based test boards: This figure has frequency as the horizontal axis and detected power as the vertical axis and is obtained by sweeping the input RF signal from 75 to 95 GHz and recording the detected power at a particular output port of the frequency processor test board shown in figure 20 above. Due to the downconverted sampling technique used by the network analyzer to measure W band signals, the 0 to 20 GHz range listed on the horizontal axis of the graph corresponds to 75 to 95 GHz in reality. In other words the W band signal at 75 to 95 GHz is down sampled to 0 to 20 GHz by oscillators internal to the network analyzer. The vertical scale is a log scale where the zero corresponds to 1 mW of RF power which by convention is written as 0 dBm. As an example, this would mean that -20 dBm would equate to 0.01 mW of power. The above graphs show that the measured peaks in the detected power agree very well the design (i.e. theoretical) peaks and that the largest sidelobe (typically adjacent to the main peak) is of the order of 10dB or less, in good agreement with what would be expected from a board operating at the diffraction limit.

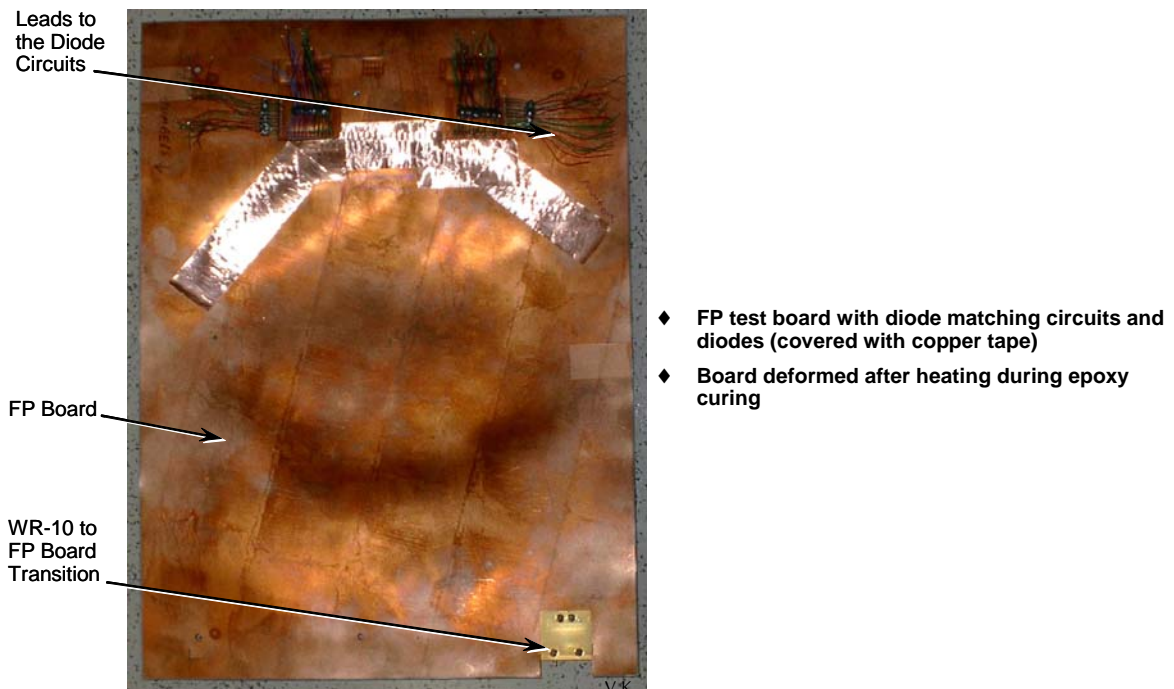


Figure 21. Full frequency processor board including W-band detector diodes. As with the phase processor, the actual signal layer is embedded between top and bottom ground planes and not evident in the photo.

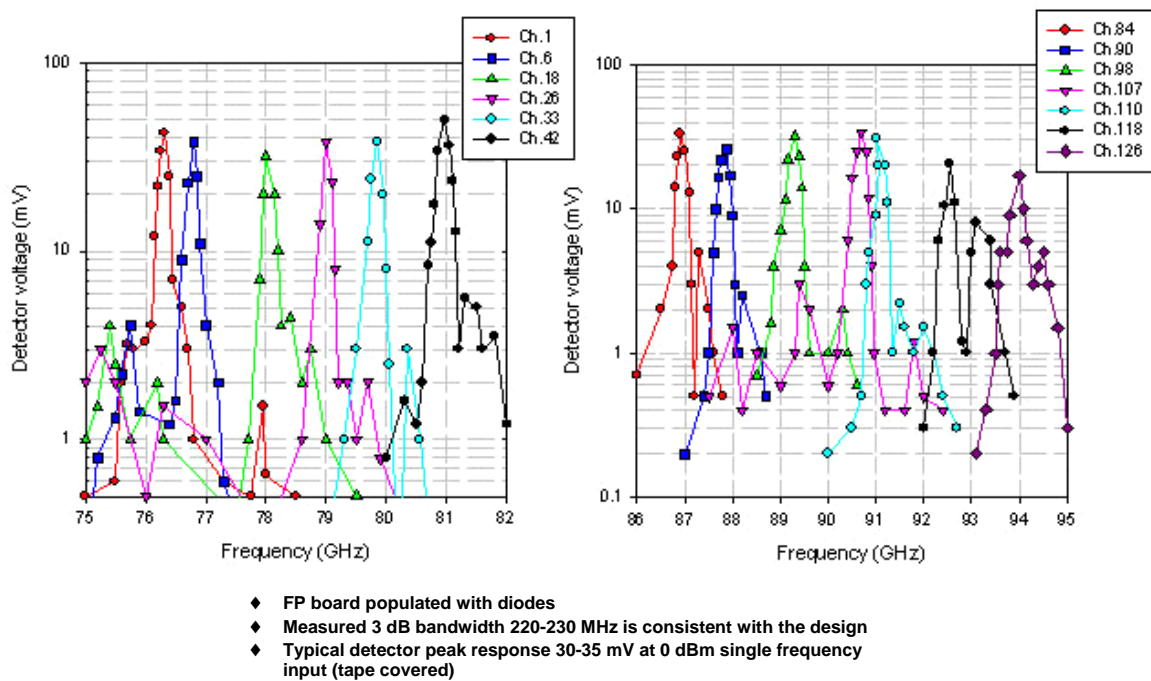
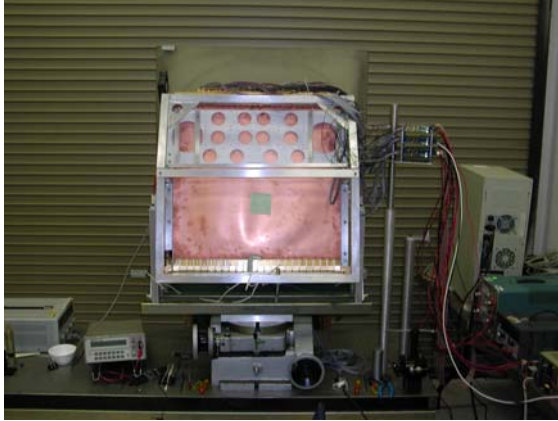


Figure 22. Response of full frequency processor board including W-band detector diodes. Note the near "sinc squared" type of response (point spread function).

While the results herein are encouraging, they indicate that some refinements to the boards are needed to achieve maximum performance.

4.0 FRONT END DEMO

Trex was tasked with performing a demonstration of the front end of the PMC-2 imager working and detecting the presence of a point source. To do this, a complete PMC-2 front end consisting of antenna, front end Octapaks, phase processor, TEKLAM mounting plate, transitions and a system support structure (SSR) or rack into which all the parts were mounted was assembled.



Front end setup in back bay for Rome demo



Side on view of front end setup

Figure 23. Images of the PMC-2 front end used for the front end demo.

As is common with all phased array imagers, radars etc, the pathlength (electrical or optical as appropriate) must be the same from all elements of the array back to where the signals are processed. Typically if the pathlength varies by more than a small fraction (approximately 0.3) of a wavelength the ability to image can be severely degraded (see Figure 18). Consequently, to ensure that PMC-2 can produce high quality near diffraction limited imagery, the pathlengths from each of the 232 input channels must be equalized. This is achieved by performing a phaseup procedure during final integration.

Electrical or optical path length is in practice adjusted by inserting into each channel a material of different electric or optical properties as appropriate for the system in question.

In the case of PMC-2, great care was taken in the design and building of the components and mounting structures such that the initial path length errors were small. Indeed measurements have shown that when left uncorrected, the errors are about $1/6^{\text{th}}$ of a wave, which while small, are not small enough to give good near diffraction limited imagery. Correction is achieved by use of high dielectric constant material that is inserted into the waveguide cavity of the transition that is used to couple the output of the antenna (after amplification by the front end Octapaks) to the input of the phase processor.

After a considerable amount of trial and error, a very repeatable procedure for determining the phase error in each channel was developed. This procedure consisted of designating a master reference channel and measuring the error of all other channels relative to this master channel. This approach is valid since in an imaging system only relative phase matters, i.e. one could add

or subtract a constant phase to ALL channels in the system without in any way changing image quality.

By turning on the RF gain in only 2 channels (the master and channel in question) at any one time ,and then rotating the imager until the power at a point near the middle of the phase processor output was maximized, the amount of phase correction for each channel could be determined. By noting the angle of rotation at which power was maximized, it was possible to extract the phase difference between the master channel and the test channel, and thereby derive the required correction.

Figure 24 below demonstrates the results of starting with the system uncompensated, after an initial phaseup at mid-band (83 GHz), and finally after a second phaseup that attempts to fine tune the initial phaseup, by averaging data over several different well spaced frequencies.

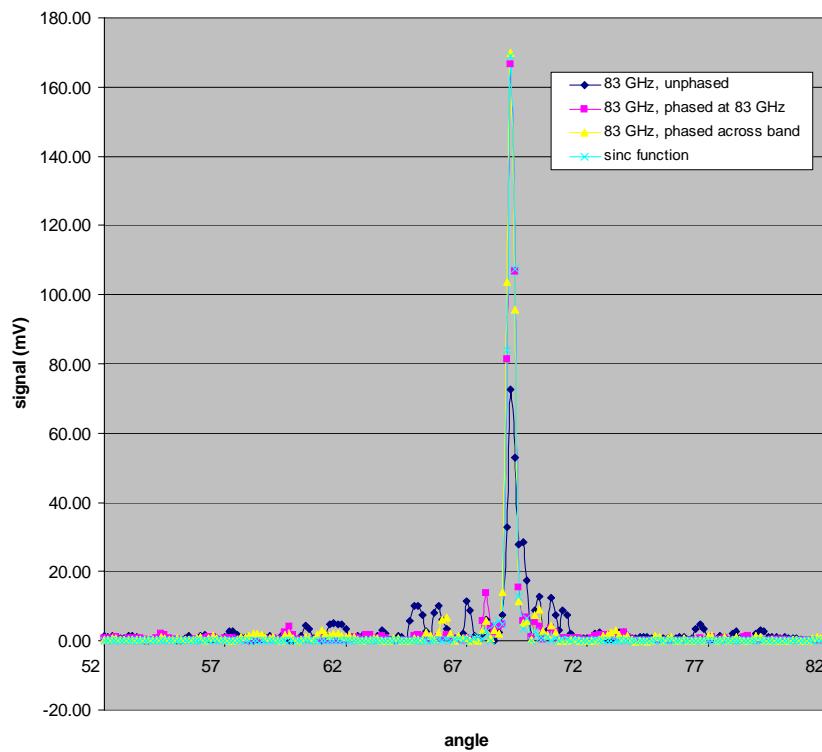


Figure 24. Before and after phaseup response functions at mid band and mid field of view.

Figures 25a through 25d, show typical post phaseup system responses, i.e. point spread functions (PSF) for a variety of positions and frequencies within the field of view. In each figure, the frequency and output port used to record the data is listed. The frequencies can vary from 75 to 93 GHz and the output port from 1 to 192.

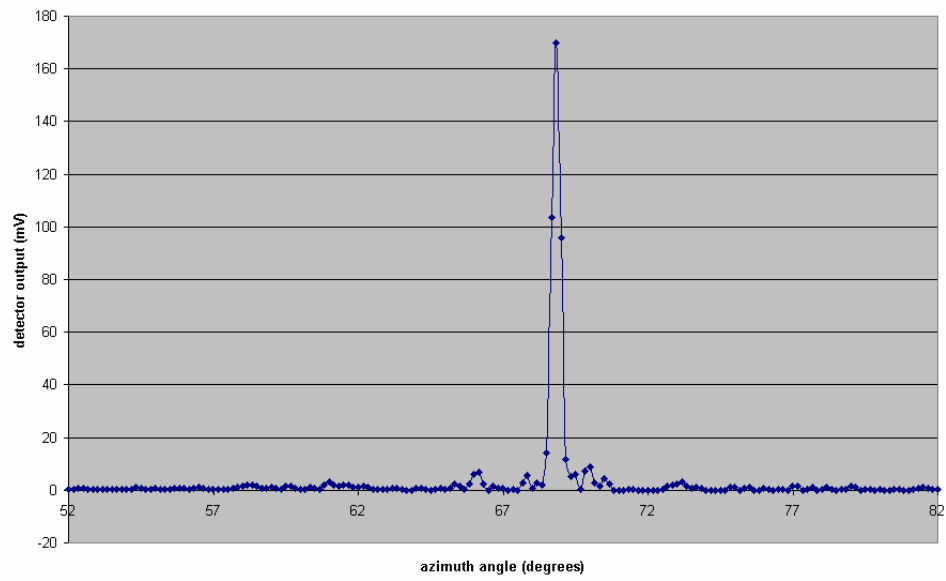


Figure 25a. Antenna pattern, $f=83$ GHz, output 112.

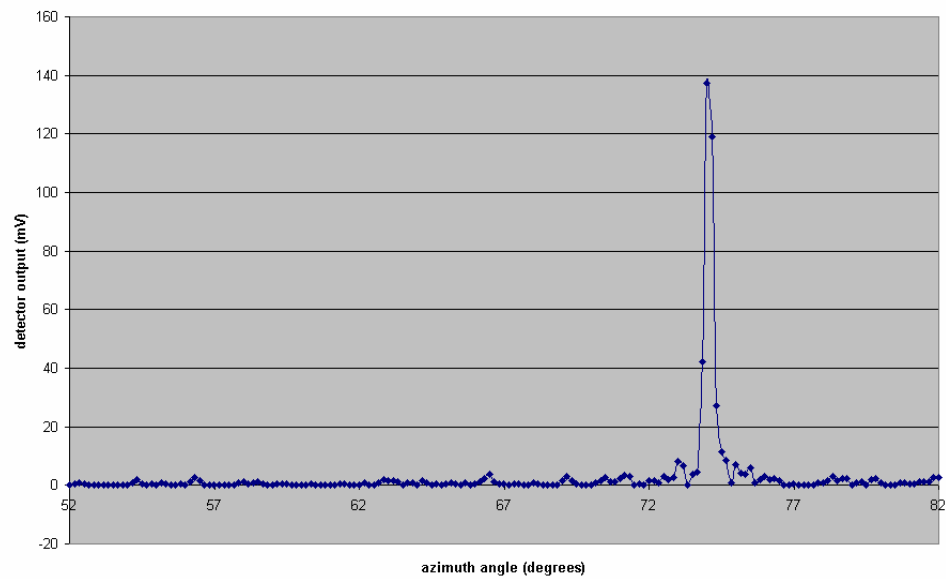


Figure 25b. Antenna pattern, $f=93$ GHz, output 145.

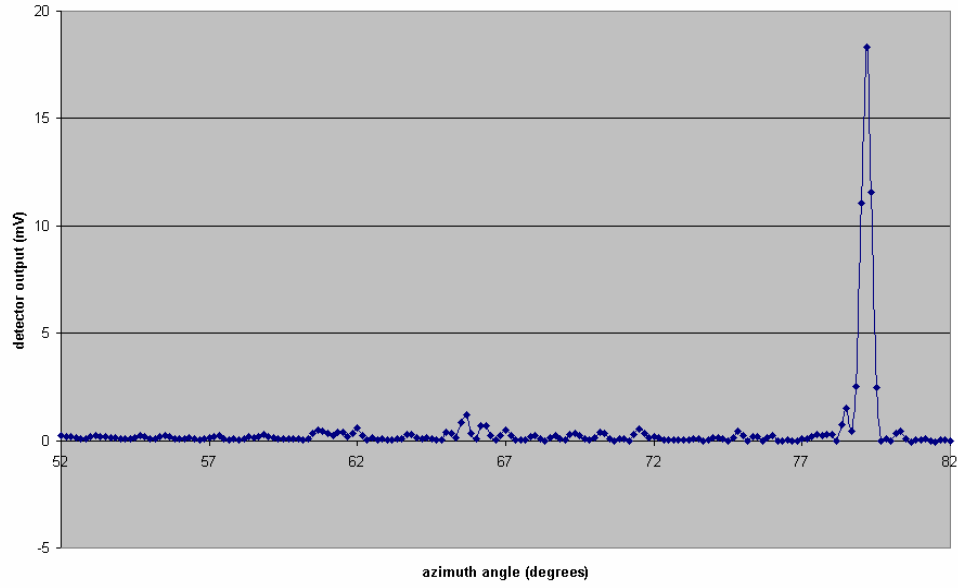


Figure 25c. Antenna pattern, $f=77$ GHz, output 169.

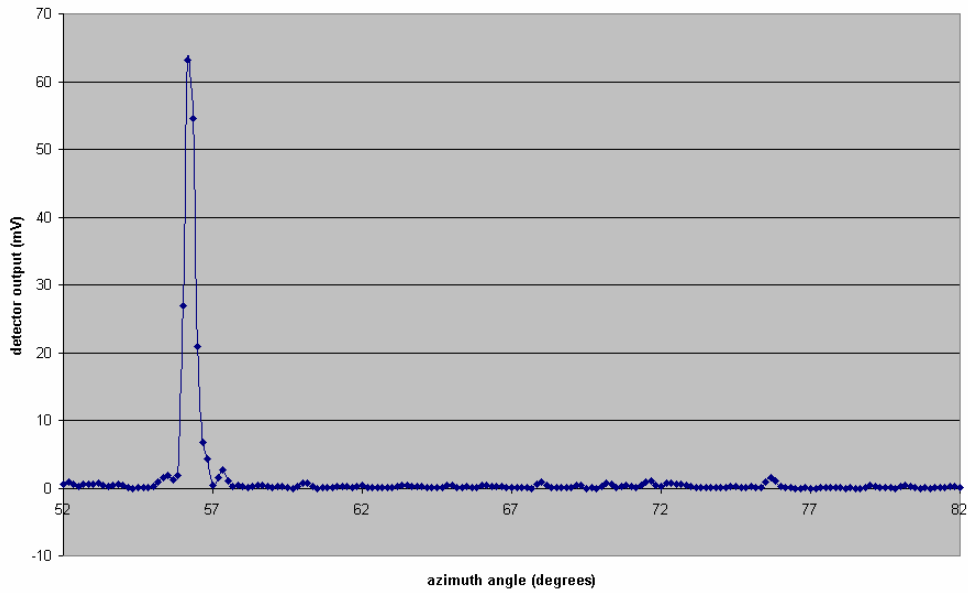


Figure 25d. Antenna pattern, $f=85$ GHz, output 33.

In each case the response is near diffraction limited such that when coupled to good frequency processors (that form the bulk of the imager back end), complete near diffraction limited 2 dimensional imaging should be possible over the full 30 by 20 degree field of view.

5.0 CONCLUSIONS

The results herein show that it is possible to achieve near diffraction limited imaging using technology developed by Trex Enterprises that produces a novel highly compact W-band passive imager.